

# Exact-exchange density functional theory for neutron drops

Joaquín E. Drut<sup>1,2</sup> and Lucas Platter<sup>3,4,2</sup>

<sup>1</sup>Theoretical Division, Los Alamos National Laboratory, Los Alamos, New Mexico 87545-0001, USA

<sup>2</sup>Department of Physics, The Ohio State University, Columbus, Ohio 43210-1117, USA

<sup>3</sup>Fundamental Physics, Chalmers University of Technology, SE-41296 Göteborg, Sweden

<sup>4</sup>Institute for Nuclear Theory, University of Washington, Seattle, Washington 98195, USA

(Received 21 April 2011; published 18 July 2011)

We compute the ground-state properties of finite systems of neutrons in an external harmonic trap, interacting via the Minnesota potential, using the “exact-exchange” form of orbital-dependent density functional theory. We compare our results with Hartree-Fock calculations and find very close agreement. Within the context of the interaction studied, we conclude that this simple orbital-dependent functional brings conventional nuclear density functional theory to the level of Hartree-Fock in an *ab initio* fashion. Our work is a first step toward higher order *ab initio* nuclear functionals based on realistic nucleon-nucleon interactions.

DOI: [10.1103/PhysRevC.84.014318](https://doi.org/10.1103/PhysRevC.84.014318)

PACS number(s): 21.60.Jz, 21.60.De, 21.65.Cd

## I. INTRODUCTION

Density functional theory (DFT) is a general theory of quantum many-body systems with a long history. In its modern version, which began with the work of Hohenberg, Kohn, and Sham [1,2], DFT has become an essential tool in quantum chemistry as well as in materials science and condensed matter physics (see, e.g., [3–5]). This is largely due to the fact that large systems, intractable by *ab initio* methods such as coupled cluster (CC) or quantum Monte Carlo (QMC) even with modern computational power, are typically within the reach of Kohn-Sham (KS) DFT with relatively modest computational resources [6]. In spite of significant progress and multiple successes, the fundamental challenge remains the same in all applications: The central object of the theory, namely the energy density functional (EDF), is *a priori* unknown and must be built either phenomenologically or from first principles (or some combination thereof) by implementing some kind of approximation scheme. Conventional DFT has slowly evolved from the first simple and often uncontrolled approximation strategies of the early days, such as Thomas-Fermi theory [7] and the local density approximation (LDA) [2], to more sophisticated semilocal approaches including the generalized gradient approximation (GGA), meta-GGAs, and hyper-GGAs [8].

Progress in the field of quantum chemistry [9] has pushed the boundaries of such conventional approaches to DFT by allowing electronic EDFs to depend explicitly on the single-particle orbitals of KS DFT. While the set of possible functionals is thus enlarged, this additional freedom comes at the price of increased formal complexity and computational demand. Indeed, the determination of the KS auxiliary one-body potential  $v_{\text{KS}}$  in the case of orbital-dependent functionals necessitates the solution of the optimized effective potential (OEP) integral equation [10,11], which prevented widespread use of these functionals for a long time. Significant advances in the last decade, however, have enabled the numerical solution of the OEP equation in a more straightforward and systematic fashion, thereby allowing orbital-dependent functionals to enter the mainstream of electronic DFT [12,13].

These developments were often motivated by the inadequacies of conventional electronic EDFs concerning some practical issues (such as their inability to deal with van der Waals forces, to predict the existence of negative ions, and to properly account for electron self-interaction [9]) as well as formal problems (such as the lack of particle-number derivative discontinuities [14] and inability to reproduce the correct long-range tail of the one-body potentials [9]). Orbital-dependent functionals have not only mitigated these issues, all of which stem from a poor description of particle exchange in GGA-based EDFs, but they have also cleared a path toward *ab initio* DFT. Indeed, many-body perturbation theory expressions for the total energy (at first order in its simplest form, i.e., Hartree-Fock, but also at second and higher orders, and in resummed forms) are generally orbital-dependent functionals, which have a clear and direct connection to the microscopic Hamiltonian [15].

Many-body systems of electrons in external fields are the standard arena for the application of DFT. However, nuclear physics shares the same interests in many-body techniques and faces very similar challenges. DFT has therefore become a standard tool for the computation of the properties of heavy nuclei. In nuclear DFT, the electrons are replaced with nucleons, and the nucleon-nucleon interaction plays the role of the Coulomb interaction. The vast majority of nuclear functionals, whether phenomenologically motivated or derived from first principles, are largely in the category of GGAs (broadly defined). The parameters in these functionals are usually fitted to a subset of stable nuclei (with the exception of some of the latest functionals, such as SLy4 or SkO, which have been fitted to some experimentally accessible unstable nuclei) and are therefore not directly related to our understanding of the nucleon-nucleon interaction.

The main objective of this work is to explore the prospects of *ab initio* DFT for the nuclear case. A more complete survey of the current status of the field can be found in Ref. [16]. In this work, we implement one of the simplest possible orbital-dependent DFTs derived from an underlying Hamiltonian, the so-called exact-exchange (EXX) form. We

apply this to the case of neutron drops interacting via the Minnesota potential [17]. We then compare the results of this DFT with exact Hartree-Fock (HF) for various numbers of neutrons in a harmonic external potential.

The EXX functional is easily defined: It consists of the HF energy, in which the single-particle HF orbitals are replaced with the KS orbitals. Thus, the fundamental difference between EXX DFT and exact HF is that at each step in the iterative optimization procedure the HF approach involves a *nonlocal* auxiliary potential, whereas KS DFT (regardless of the form of the functional) utilizes a *local* auxiliary potential  $v_{\text{KS}}$ . (It remains an open question whether such local auxiliary field will be too constraining for nuclear physics; see, e.g., Ref. [18].) In this sense, EXX DFT can be regarded as a constrained optimization of the HF energy, where the constraint consists in demanding the locality of  $v_{\text{KS}}$ . As a consequence, the ground-state energies obtained via EXX DFT should be expected to be higher than those of HF. As we shall see, the differences are very small in the case we study, but this will in general depend on the form of the interaction.

While EXX DFT is formally simple, we do not claim that it is accurate in an absolute sense, but rather that it represents an extremely accurate approximation to exact HF. As mentioned above, this property will in general depend on the interaction. However, we wish to stress this point as a promising feature of orbital-dependent DFT, even though HF calculations are well known to be a poor description of nuclei due to the nonperturbative nature of the nuclear interaction at short distances (cf. high momenta). A more realistic description must both transcend perturbation theory and include pairing correlations at least at the mean-field level, i.e., à la Hartree-Fock-Bogoliubov (HFB). Work in this direction has recently involved efforts toward taming the nuclear interaction at high momenta using renormalization group (RG) transformations [19].<sup>1</sup> These are transformations that leave observables unchanged but reduce the strength of the potential at large momenta. Such transformations render the problem more perturbative while maintaining the hierarchy of many-body forces. In this context, our work may be regarded as a necessary first step in an *ab initio* DFT program that connects microscopic RG-transformed Hamiltonians with orbital-dependent DFT based on HFB plus perturbation theory.

## II. KOHN-SHAM DFT AND THE OPTIMIZED EFFECTIVE POTENTIAL

In quantum chemistry, the “optimized potential method,” or simply the “optimized effective potential,” refers collectively to the use of orbital-dependent EDFs and to the determination of the KS auxiliary potential  $v_{\text{KS}}$  by solving the OEP integral equation. For completeness, and in order to set our notation, we present here a short derivation of this equation, along with a brief review of KS DFT. For simplicity, we shall

<sup>1</sup>A possible alternative approach would be to employ directly chiral effective theory interactions that are soft by construction [20].

restrict ourselves to functionals that do not depend on the KS eigenvalues; the corresponding generalization is easy to carry out.

### A. Derivation of the OEP equation

The central tenet of DFT is the Hohenberg-Kohn (HK) theorem, whereby the existence of an energy density functional is asserted, of the form

$$E[\rho] = F[\rho] + E_{\text{ext}}[\rho], \quad (1)$$

where

$$E_{\text{ext}}[\rho] = \int d\mathbf{x} v_{\text{ext}}(\mathbf{x})\rho(\mathbf{x}), \quad (2)$$

such that  $F[\rho]$  depends only on the one-body density  $\rho(\mathbf{x})$ . One may think of the latter as the total density, but in general it may denote spin, isospin, kinetic, or anomalous densities, in which case  $\mathbf{x}$  represents a collective index for the coordinate and every other degree of freedom.

The external potential  $v_{\text{ext}}$  represents the electric field of the ions, and it confines the system to a particular spatial region. This is a fundamental difference between the electronic and nuclear cases, since in the latter the system is self-bound; i.e., there is no  $v_{\text{ext}}$  [16].

According to the HK theorem, the functional form of  $F$  is determined solely by the interactions and not by the external potential  $v_{\text{ext}}$ ; the functional  $F$  is therefore said to be *universal*. The HK theorem is an existence theorem and gives therefore no instructions as to how to build or find this functional. Kohn-Sham DFT takes a first formal step toward the explicit construction of  $F[\rho]$  by separating it into a noninteracting piece, i.e., the kinetic energy of the free system, and everything else:

$$F[\rho] = T_s + E_{\text{int}}[\rho], \quad (3)$$

where

$$T_s = \sum_{\sigma=\uparrow,\downarrow} \sum_{k=1}^{N_{\sigma}} \int d\mathbf{x} \varphi_{k\sigma}^*(\mathbf{x}) \left( -\frac{\hbar^2 \nabla^2}{2m} \right) \varphi_{k\sigma}(\mathbf{x}). \quad (4)$$

It should be stressed that  $T_s$  represents the kinetic energy of the auxiliary KS system, which in general is different from that of the many-body system. Their difference is assumed to be accounted for in  $E_{\text{int}}[\rho]$ .

The  $\varphi_{k\sigma}(\mathbf{x})$  are a set of auxiliary single-particle orbitals (the KS orbitals), such that  $\rho = \rho_{\uparrow} + \rho_{\downarrow}$ , where

$$\rho_{\sigma}(\mathbf{x}) = \sum_{k=1}^{N_{\sigma}} |\varphi_{k\sigma}(\mathbf{x})|^2, \quad (5)$$

and  $N_{\sigma}$  is the particle number for spin  $\sigma$ . Kohn-Sham DFT then proceeds to optimize the energy functional by solving a Schrödinger-like equation:

$$\left[ -\frac{\hbar^2 \nabla^2}{2m} + v_{\text{KS},\sigma}(\mathbf{x}) \right] \varphi_{k\sigma}(\mathbf{x}) = \epsilon_k \varphi_{k\sigma}(\mathbf{x}), \quad (6)$$

for all  $k$ . As mentioned above, this should be contrasted with the HF approximation, in which the corresponding

Schrödinger equation involves a nonlocal potential. In this sense, EXX DFT can be regarded as resulting from an HF minimization procedure, with the added constraint that the auxiliary potential be local. In spite of this constraint, orbital-dependent DFT beyond EXX has the potential to surpass HF, and in fact does so in practice in the electronic case (see, e.g., Ref. [9]).

By definition, the KS potential in Eq. (6) is given by

$$v_{\text{KS},\sigma}(\mathbf{x}) \equiv \frac{\delta V}{\delta \rho_\sigma(\mathbf{x})} = v_{\text{ext}}(\mathbf{x}) + \frac{\delta E_{\text{int}}}{\delta \rho_\sigma(\mathbf{x})}, \quad (7)$$

where

$$V \equiv E_{\text{ext}} + E_{\text{int}}. \quad (8)$$

The second term on the rhs of Eq. (7) will in general depend on the KS orbitals, such that Eq. (6) is to be solved self-consistently by starting with a guess for the orbitals or for  $v_{\text{KS}}$ .

It is at this point that orbital-dependent DFT departs from GGA DFT, in which functionals depend *explicitly* on the density and its gradients. Indeed, once we allow  $E_{\text{int}}$  to depend *explicitly* on the KS orbitals, it becomes unclear how to determine the KS potential using its definition Eq. (7). One of the simplest ways to proceed is to use the chain rule of functional differentiation and consider the following identity:

$$\frac{\delta V}{\delta v_{\text{KS},\sigma}(\mathbf{x})} = \sum_{\sigma'=\uparrow,\downarrow} \sum_{k=1}^{N_\sigma} \int d\mathbf{y} \frac{\delta V}{\delta \varphi_{k\sigma'}(\mathbf{y})} \frac{\delta \varphi_{k\sigma'}(\mathbf{y})}{\delta v_{\text{KS},\sigma}(\mathbf{x})} + \text{c.c.} \quad (9)$$

In order to proceed we vary both sides of the eigenvalue equation Eq. (6) (and its complex conjugate):

$$\frac{\delta \varphi_{k\sigma}(\mathbf{y})}{\delta v_{\text{KS},\sigma}(\mathbf{x})} = G_k^{\sigma'\sigma}(\mathbf{y}, \mathbf{x}) \varphi_{k\sigma}(\mathbf{x}), \quad (10)$$

where

$$G_k^{\sigma'\sigma}(\mathbf{y}, \mathbf{x}) = \delta_{\sigma\sigma'} G_{k\sigma}(\mathbf{y}, \mathbf{x}), \quad (11)$$

with

$$G_{k\sigma}(\mathbf{y}, \mathbf{x}) = \sum_{q \neq k} \frac{\varphi_q^*(\mathbf{x}) \varphi_{q\sigma}(\mathbf{y})}{\epsilon_k - \epsilon_q} \quad (12)$$

being the Green's function. Equation (9) then becomes

$$\frac{\delta V}{\delta v_{\text{KS},\sigma}(\mathbf{x})} = \sum_{k=1}^{N_\sigma} \int d\mathbf{y} \frac{\delta V}{\delta \varphi_{k\sigma}(\mathbf{y})} G_{k\sigma}(\mathbf{y}, \mathbf{x}) \varphi_{k\sigma}(\mathbf{x}) + \text{c.c.} \quad (13)$$

On the other hand, the HK theorem allows us to take implicit derivatives with respect to the density  $\rho_\sigma(\mathbf{x})$ :

$$\begin{aligned} \frac{\delta V}{\delta v_{\text{KS},\sigma}(\mathbf{x})} &= \int d\mathbf{x}_1 \frac{\delta V}{\delta \rho_\sigma(\mathbf{x}_1)} \frac{\delta \rho_\sigma(\mathbf{x}_1)}{\delta v_{\text{KS},\sigma}(\mathbf{x})} \\ &= \int d\mathbf{x}_1 v_{\text{KS},\sigma}(\mathbf{x}_1) \frac{\delta \rho_\sigma(\mathbf{x}_1)}{\delta v_{\text{KS},\sigma}(\mathbf{x})} \\ &= \sum_{k=1}^{N_\sigma} \int d\mathbf{x}_1 v_{\text{KS},\sigma}(\mathbf{x}_1) \varphi_{k\sigma}^*(\mathbf{x}_1) G_{k\sigma}(\mathbf{x}_1, \mathbf{x}) \varphi_{k\sigma}(\mathbf{x}), \\ &\quad + \text{c.c.}, \end{aligned} \quad (14)$$

where we have used Eqs. (5) and (7). Combining Eqs. (13) and (14) we arrive at

$$\sum_{k=1}^{N_\sigma} [\psi_{k\sigma}^*(\mathbf{x}) \varphi_{k\sigma}(\mathbf{x}) + \text{c.c.}] = 0, \quad (15)$$

where we have defined the “orbital shift”  $\psi_{k\sigma}$  by

$$\begin{aligned} \psi_{k\sigma}^*(\mathbf{x}) \equiv & \int d\mathbf{x}_1 \left[ \frac{\delta V}{\delta \varphi_{k\sigma}(\mathbf{x}_1)} - v_{\text{KS},\sigma}(\mathbf{x}_1) \varphi_{k\sigma}^*(\mathbf{x}_1) \right] \\ & \times G_{k\sigma}(\mathbf{x}_1, \mathbf{x}). \end{aligned} \quad (16)$$

Equation (15) is the OEP integral equation that defines the KS potential of orbital-based DFT.

## B. Solving the OEP equation

While there are in principle multiple ways to solve the OEP equation, we have found the one originally due to Kümmel and Perdew [13] to be particularly useful. We shall refer to this method as the Kümmel-Perdew (KP) algorithm. This algorithm is iterative and starts by noting that the orbital shifts can be found by solving a differential equation, namely

$$\left[ -\frac{\hbar^2 \nabla^2}{2m} + v_{\text{KS},\sigma}(\mathbf{x}) - \epsilon_k \right] \psi_{k\sigma}^*(\mathbf{x}) = \Lambda_{k\sigma}(\mathbf{x}) \varphi_{k\sigma}^*(\mathbf{x}) \quad (17)$$

and

$$\begin{aligned} \Lambda_{k\sigma}(\mathbf{x}) \equiv & v_{\text{KS},\sigma}(\mathbf{x}) - u_{k\sigma}(\mathbf{x}) \int d\mathbf{x}_1 [v_{\text{KS},\sigma}(\mathbf{x}_1) \\ & - u_{k\sigma}(\mathbf{x}_1)] \varphi_{k\sigma}^*(\mathbf{x}_1) \varphi_{k\sigma}(\mathbf{x}_1), \end{aligned} \quad (18)$$

with

$$u_{k\sigma}(\mathbf{x}) \equiv \frac{1}{\varphi_{k\sigma}^*(\mathbf{x})} \frac{\delta V}{\delta \varphi_{k\sigma}(\mathbf{x})}, \quad (19)$$

where we assume some form for the initial  $v_{\text{KS},\sigma}(\mathbf{x})$ . Once the orbital shifts are determined,  $v_{\text{KS},\sigma}$  is updated according to

$$v_{\text{KS},\sigma}^{\text{new}}(\mathbf{x}) = v_{\text{KS},\sigma}^{\text{old}}(\mathbf{x}) + c S_\sigma(\mathbf{x}), \quad (20)$$

where  $c$  is a positive constant and the function

$$S_\sigma(\mathbf{x}) \equiv \sum_{k=1}^{N_\sigma} [\psi_{k\sigma}^*(\mathbf{x}) \varphi_{k\sigma}(\mathbf{x}) + \text{c.c.}] \quad (21)$$

[cf. Eq. (15)] is used as a local measure of the deviation of the current  $v_{\text{KS}}$  with respect to the true solution of the OEP equation. Indeed, wherever  $v_{\text{KS},\sigma}(\mathbf{x})$  differs from the true OEP,  $S_\sigma(\mathbf{x})$  will be nonzero. The updated  $v_{\text{KS}}$  can be used to recompute the orbital shifts, keeping the KS orbitals and eigenvalues constant, until the desired convergence criterion is satisfied. The final  $v_{\text{KS}}$  is then reinserted in the KS equation (6) to compute a new set of orbitals, closing the self-consistency loop.

It is easy to see that Eq. (17) is singular. Adding any multiple of  $\varphi_{k\sigma}(\mathbf{x})$  to  $\psi_{k\sigma}^*(\mathbf{x})$  gives a new nontrivial solution. As first noted in Ref. [13], however, Eq. (17) can still be solved in the subspace of interest by using the method of conjugate

gradients [21]. Further details of this approach can be found in Ref. [13].

The determination of the orbital shifts  $\psi_{k\sigma}^*$  via Eq. (17) represents an additional computational cost that is not present in LDA- or GGA-based DFT. Indeed, in the latter  $v_{KS,\sigma}$  is determined simply by inserting the density and its gradients in a precalculated analytic expression derived from the EDF via Eq. (7). In contrast, in the OEP method (within the KP approach) the calculation of all the  $\psi_{k\sigma}^*$ 's necessitates the solution of  $N$  differential equations, where  $N$  is the number of particles. While this is a considerable increase in computational demand, it should be kept in mind that the  $\psi_{k\sigma}^*$ 's are independent from each other, such that the  $N$  differential equations can be solved in a parallel fashion with perfect scaling [up to communication costs required to broadcast  $v_{KS}(\mathbf{x})$  at the beginning and to compute  $S_\sigma(\mathbf{x})$  at the end].

### III. EXX ENERGY DENSITY FUNCTIONAL AND THE MINNESOTA POTENTIAL

We have used in this work the Minnesota nucleon-nucleon interaction of Ref. [17], which is given for pure neutron systems by

$$V(r) = [V_R(r) + V_s(r)\mathcal{P}_s + V_t(r)\mathcal{P}_t]\frac{1}{2}(1 + P^r), \quad (22)$$

where  $\mathcal{P}_s$  ( $\mathcal{P}_t$ ) is the operator that projects on the spin singlet (triplet) state and  $P^r$  is the coordinate exchange operator. The potentials in the various channels have Gaussian forms given by

$$\begin{aligned} V_R &= V_{0R} \exp(-\kappa_R r^2), \\ V_t &= -V_{0t} \exp(-\kappa_t r^2), \\ V_s &= -V_{0s} \exp(-\kappa_s r^2) \end{aligned} \quad (23)$$

and

$$\begin{aligned} V_{0R} &= 200.0 \text{ MeV}, & \kappa_R &= 1.487 \text{ fm}^{-2}, \\ V_{0t} &= 178.0 \text{ MeV}, & \kappa_t &= 0.639 \text{ fm}^{-2}, \\ V_{0s} &= 91.85 \text{ MeV}, & \kappa_s &= 0.465 \text{ fm}^{-2}. \end{aligned} \quad (24)$$

Our main reason for using this potential is that it provides a semirealistic yet easy-to-implement interaction. In addition, this potential is moderately soft and as such it is comparable to those obtained using renormalization-group methods [19]. Other approaches to *ab initio* DFT are also being explored using this simple potential, and no-core-full-configuration (NCFC) and coupled-cluster (CC) results have recently become available as well, which makes this a good test case for OEP methods.

The energy density functional is of the form given in Eq. (3) and the mass in the kinetic energy term [Eq. (3)] has been set to  $m_n = 939$  MeV. In practice, one combines the kinetic term with the external harmonic oscillator (HO) potential energy. This is convenient because the KS orbitals can be expanded

using the HO basis  $\{\phi_j\}$ ,

$$\varphi_{k\sigma}(\mathbf{x}) = \sum_{j=1}^{N_{\max}} a_{jk,\sigma} \phi_j(\mathbf{x}), \quad (25)$$

$$a_{jk,\sigma} = \int d\mathbf{x} \phi_j^*(\mathbf{x}) \varphi_{k\sigma}(\mathbf{x}), \quad (26)$$

and in this basis the sum  $T_s + E_{\text{ext}}$  takes a simple diagonal form.

In the EXX case considered in this work the interaction enters through

$$E_{\text{int}} = \frac{1}{2} \sum_{ijkl} \bar{V}_{ijkl} \rho_{ki} \rho_{lj}, \quad (27)$$

where we have used collective indices  $i$  to denote the pair  $(i, \sigma_i)$  for the basis element and the spin. Here,

$$\rho_{ij} \equiv \rho_{i\sigma_i; j\sigma_j} = \delta_{\sigma_i \sigma_j} \sum_{k=1}^{N_\sigma} a_{ik, \sigma_i}^* a_{jk, \sigma_i} \quad (28)$$

is the one-body density matrix, and

$$\bar{V}_{ijkl} = V_{ijkl} - V_{ijlk} \quad (29)$$

are the antisymmetrized matrix elements of the interaction. As mentioned above, this form of  $F[\rho]$  is simply that of the HF energy, but with the KS orbitals replacing the HF single-particle wave functions. The interaction in Eq. (23) is local and we therefore obtain

$$V_{ijkl} = \int d\mathbf{x}_1 d\mathbf{x}_2 \phi_i^*(\mathbf{x}_1) \phi_j^*(\mathbf{x}_2) V(r) \phi_k(\mathbf{x}_1) \phi_l(\mathbf{x}_2), \quad (30)$$

where  $r = |\mathbf{x}_1 - \mathbf{x}_2|$  and the total spin of the initial  $(ik)$  and final  $(jl)$  states is the same.

### IV. RESULTS AND CONCLUSIONS

We have considered systems of 8 and 20 neutrons for various trap frequencies and basis sizes, and computed the total energy

$$E_{\text{tot}} = E_{\text{kin}} + U_{\text{ext}} + E_{\text{H}} + E_{\text{F}}, \quad (31)$$

where  $E_{\text{kin}} = T_s$  and

$$U_{\text{ext}} = \int d\mathbf{x} v_{\text{ext}}(\mathbf{x}) \rho(\mathbf{x}), \quad (32)$$

where

$$v_{\text{ext}}(\mathbf{x}) = \frac{1}{2} m_n \Omega^2 \mathbf{x}^2 \quad (33)$$

is the HO external potential.

The total energy can also be obtained from eigenvalue sum rules, which we have verified numerically, and are given in the HF case by

$$E_{\text{tot}} = \sum_{k,\sigma} \epsilon_k - E_{\text{H}} - E_{\text{F}}, \quad (34)$$

where each term is evaluated using HF orbitals, and in the EXX-DFT case by

$$E_{\text{tot}} = \sum_{k,\sigma} \epsilon_k + E_H + E_F - \sum_{\sigma} \int d\mathbf{x} v_{\text{KS},\sigma}(\mathbf{x}) \rho_{\sigma}(\mathbf{x}), \quad (35)$$

where the EXX-DFT orbitals should be used. Notice that in both sum rules the eigenvalue sums go over both spins. The Hartree and Fock energies are respectively given by

$$E_H = \frac{1}{2} \sum_{ijkl} V_{ijkl} \rho_{ki} \rho_{lj}, \quad (36)$$

$$E_F = -\frac{1}{2} \sum_{ijkl} V_{ijkl} \rho_{ki} \rho_{lj}. \quad (37)$$

We have also computed the rms radius  $\sqrt{\langle r^2 \rangle}$ , where

$$\langle r^2 \rangle = \frac{1}{N} \int d\mathbf{x} r^2 \rho(r), \quad (38)$$

as well as the form factor, given by

$$F(q) = 4\pi \int dr r^2 \rho(r) \frac{\sin qr}{qr}, \quad (39)$$

where  $q = |\mathbf{q}|$  and  $r = |\mathbf{x}|$ .

Our results for the internal energy  $E_{\text{tot}} - U_{\text{ext}}$  per particle, as a function of the rms radius, are shown in Fig. 1, for various frequencies of the trapping potential. Also shown in Fig. 1 are the results corresponding to 8 and 20 neutrons, and in all cases we display the degree of convergence of HF and EXX DFT, with respect to the size of the basis  $N_{\text{max}}$ , by showing data for  $N_{\text{max}} = 64, 125$ , and 216. Figures 2 and 3 show the density profiles and the corresponding form factors for a fixed external harmonic potential of frequency  $\hbar\Omega = 10$  MeV and basis size  $N_{\text{max}} = 27, 64, 125$ , and 216. Throughout this work we have chosen the value of  $\hbar\Omega$  for the basis equal to that of the trapping potential. As seen in the plots, in all cases the convergence pattern of HF and EXX DFT as a function of  $N_{\text{max}}$

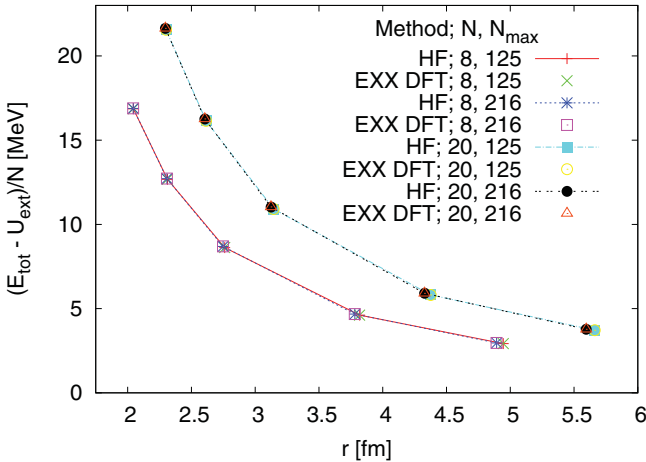


FIG. 1. (Color online) Internal energy as a function of the rms radius for 8 (lower curve) and 20 (upper curve) neutrons, computed with HF and EXX DFT, for two different basis sizes, namely  $N_{\text{max}} = 125$  and 216. From left to right, the trapping potential corresponds to  $\hbar\Omega = 20, 15, 10, 5$ , and 3 MeV.

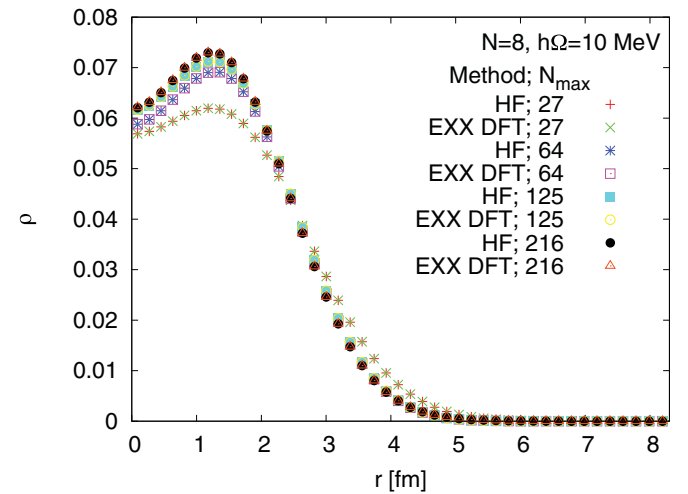


FIG. 2. (Color online) Density profiles of a system of 8 neutrons in a  $\hbar\Omega = 10$  MeV trap as a function of the basis size  $N_{\text{max}}$ , computed with HF and EXX DFT.

is the same. At fixed  $N_{\text{max}}$ , on the other hand, the convergence patterns as a function of the respective HF and KS iterations are significantly different from each other. We provide a partial summary of our results in Table I.

We have implemented a parallel code (using OpenMP) for both the HF and OEP calculations. The latter use some of the HF routines and a set of extra ones to solve the OEP equations. Using 8 processors and some limited optimizations of the parameters (such as the constant  $c$  in the KP algorithm and the number of iterations in the KP loop) we have found that, at fixed accuracy for the convergence criterion, OEP calculations require about a factor of 2–3 more iterations than HF, and each OEP iteration takes about a factor of 2–3 more time than its HF counterpart, for the basis sizes and particle numbers studied here. Thus, overall the OEP method at the EXX-DFT level is a factor of 4–9 slower than HF. However, further optimizations are possible if for example MPI is used in the parallelization of the calculation of the orbital shifts. This

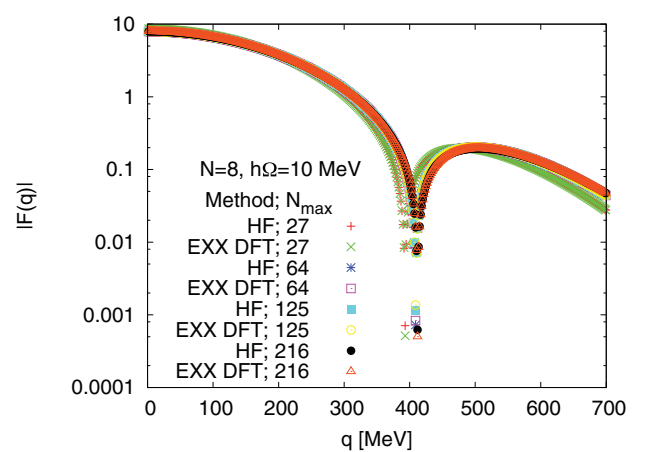


FIG. 3. (Color online) Form factor of a system of 8 neutrons in a  $\hbar\Omega = 10$  MeV trap as a function of the basis size  $N_{\text{max}}$ , computed with HF and EXX DFT.

TABLE I. Summary of results for the energies in MeV for Hartree-Fock (HF) and exact-exchange DFT (EXX), broken up into total ( $E_{\text{tot}}$ ), kinetic ( $E_{\text{kin}}$ ), Hartree ( $E_{\text{H}}$ ), Fock ( $E_{\text{F}}$ ), and internal ( $E_{\text{I}} = E_{\text{tot}} - U_{\text{ext}}$ ). Also shown is the rms radius  $\sqrt{\langle r^2 \rangle}$ .

Method	$N$	$\hbar\Omega$	$E_{\text{tot}}$	$E_{\text{kin}}$	$E_{\text{H}}$	$E_{\text{F}}$	$E_{\text{I}}$	$\sqrt{\langle r^2 \rangle}$
HF	8	20	296.36	200.92	-225.18	159.35	135.09	2.0438
EXX	8	20	296.36	200.99	-225.24	159.39	135.14	2.0435
HF	8	10	142.43	111.22	-125.38	83.70	69.53	2.7484
EXX	8	10	142.44	111.27	-125.44	83.74	69.56	2.7478
HF	8	3	44.51	35.18	-30.51	19.05	23.72	4.8927
EXX	8	3	44.51	35.19	-30.52	19.05	23.72	4.8921
HF	20	20	941.75	707.69	-920.03	645.08	432.74	2.2965
EXX	20	20	941.77	707.83	-920.19	645.20	432.84	2.2963
HF	20	10	456.25	382.73	-488.61	326.55	220.68	3.1246
EXX	20	10	456.26	382.88	-488.80	326.69	220.77	3.1240
HF	20	3	143.52	119.55	-118.19	74.15	75.52	5.5958
EXX	20	3	143.52	119.57	-118.21	74.17	75.53	5.5954

would have significant impact in calculations for larger particle number and larger basis size, as well as for more sophisticated functionals.

## V. SUMMARY AND OUTLOOK

In this work we have computed the energy, radius, density profile, and form factor of finite systems of neutrons in a harmonic trap. For this purpose we have used pure HF and orbital-based DFT in the EXX form, implementing the algorithm of Kümmel and Perdew to solve the OEP equation. Our results for the OEP approach agree at the 0.1% level or better with those of pure HF for all the quantities we computed. We note in particular that such an agreement was reached for each basis size even though HF and OEP converge to their respective results in completely different ways. Although limited in scope, our work shows that it is possible to capture the exchange aspects of the nuclear interaction in an extremely accurate fashion completely within the context of local KS-DFT.

As mentioned in the introduction, this work represents the first step in a program whose objective is to construct a nuclear energy density functional from first principles, employing orbital-based methods. Ideally, this functional would be able to at least qualitatively predict the properties of heavy nuclei and would only be based on our microscopic understanding of the internucleon interaction. We do not exclude the possibility, however, that an accurate quantitative description of energies and radii may require readjusting certain parameters in this functional. In this sense, our work is a step forward from LDA- and GGA-based DFTs, which are typically phenomenological in nature in the nuclear case, and therefore limited in their

ability to predict the properties of unknown systems. Much work remains to be done, however, to bring this approach to a level of accuracy that is competitive with state-of-the-art nuclear EDFs.

Orbital-based DFT is one possible road out among several currently pursued in the nuclear DFT community. An alternative way is to find a controlled scheme that approximates the nonlocal *ab initio* functional with a local one and thereby facilitates the application of standard KS DFT (see, e.g., [22]).

The next step in this *ab initio* DFT program will be to treat nuclei by implementing realistic nuclear interactions such as chiral interactions softened with modern renormalization group methods. This will require extending the current framework to include many-body forces and noncentral as well as nonlocal terms in the interaction. This is currently underway; we have successfully performed proof-of-principle calculations with three-body forces, and shown that the formalism for many-body forces at the EXX level is a straightforward extension of our presentation in Sec. II [23]. Extensions of the OEP method currently in progress involve improved functionals, e.g., those generated by second-order perturbation theory, as well as modifications to account for pairing correlations.

## ACKNOWLEDGMENTS

We acknowledge support under US DOE Grants No. DE-FG02-00ER41132 and DE-AC02-05CH11231, UNEDF SciDAC Collaboration Grant No. DE-FC02-07ER41457, and NSF Grant No. PHY-0653312, and from the Swedish Research Council. We would like to thank E. R. Anderson, S. K. Bogner, R. J. Furnstahl, and K. Hebeler for useful discussions.

- 
- [1] P. Hohenberg and W. Kohn, *Phys. Rev.* **136**, B864 (1964).  
[2] W. Kohn and L. J. Sham, *Phys. Rev.* **140**, A1133 (1965).  
[3] R. M. Dreizler and E. K. U. Gross, *Density Functional Theory* (Springer, Berlin, 1990).  
[4] R. G. Parr and W. Yang, *Density Functional Theory of Atoms and Molecules* (Oxford University Press, 1994).  
[5] J. Kohanoff, *Electronic Structure Calculations for Solids and Molecules: Theory and Computational Methods* (Cambridge University Press, 2006).

- [6] W. Kohn, *Rev. Mod. Phys.* **71**, 1253 (1999); J. A. Pople, *ibid.* **71**, 1267 (1999).
- [7] L. H. Thomas, *Proc. Cambridge Philos. Soc.* **23**, 542 (1927); E. Fermi, *Z. Phys.* **48**, 73 (1928).
- [8] J. P. Perdew and K. Schmidt, in *Density Functional Theory and Its Applications to Materials*, edited by V. E. Van Doren, K. Alsenoy, and P. Geerlings (American Institute of Physics, Melville, NY, 2001); J. Perdew and S. Kurth, in *A Primer in Density Functional Theory*, edited by C. Fiolhais, F. Nogueira, and M. Marques (Springer, Berlin, 2003), pp. 1–55; J. P. Perdew *et al.*, *J. Chem. Phys.* **123**, 062201 (2005).
- [9] E. Engel, in *A Primer in Density Functional Theory*, edited by C. Fiolhais, F. Nogueira, and M. Marques (Springer, Berlin, 2003); S. Kümmel and L. Kronik, *Rev. Mod. Phys.* **80**, 3 (2008).
- [10] R. T. Sharp and G. K. Horton, *Phys. Rev.* **90**, 317 (1953); J. D. Talman and W. F. Shadwick, *Phys. Rev. A* **14**, 36 (1976); V. Sahni, J. Gruenebaum, and J. P. Perdew, *Phys. Rev. B* **26**, 4371 (1982).
- [11] S. Kurth and S. Pittalis, in *Computational Nanoscience*, edited by J. Grotendorst, S. Blugel, and D. Marx, NIC Series 31 (John von Neumann Institute for Computing, Julich, Germany, 2006), p. 299.
- [12] A. Görling and M. Levy, *Phys. Rev. A* **50**, 196 (1994); A. Görling, *Phys. Rev. Lett.* **83**, 5459 (1999).
- [13] S. Kümmel and J. P. Perdew, *Phys. Rev. Lett.* **90**, 043004 (2003); *Phys. Rev. B* **68**, 035103 (2003).
- [14] J. P. Perdew *et al.*, *Phys. Rev. Lett.* **49**, 1691 (1982).
- [15] R. J. Bartlett, V. F. Lotrich, and I. V. Schweigert, *J. Chem. Phys.* **123**, 062205 (2005).
- [16] J. E. Drut, R. J. Furnstahl, and L. Platter, *Prog. Part. Nucl. Phys.* **64**, 120 (2010).
- [17] D. R. Thompson, M. Lemere, and Y. C. Tang, *Nucl. Phys. A* **286**, 53 (1977).
- [18] T. Duguet *et al.*, arXiv:nucl-th/0606037; T. Duguet and T. Lesinski (unpublished); T. Duguet *et al.*, *AIP Conf. Proc.* **1165**, 243 (2009).
- [19] S. K. Bogner, R. J. Furnstahl, and A. Schwenk, *Prog. Part. Nucl. Phys.* **65**, 94 (2010).
- [20] L. Coraggio, A. Covello, A. Gargano, N. Itaco, D. R. Entem, T. T. S. Kuo, and R. Machleidt, *Phys. Rev. C* **75**, 024311 (2007).
- [21] M. R. Hestenes, E. Stiefel, and J. Res, *Natl. Bur. Stand.* **49**, 409 (1952); W. H. Press *et al.*, *Numerical Recipes in FORTRAN*, 2nd ed. (Cambridge University Press, Cambridge, 1992).
- [22] J. W. Negele and D. Vautherin, *Phys. Rev. C* **5**, 1472 (1972); **11**, 1031 (1975); S. K. Bogner, R. J. Furnstahl, and L. Platter, *Eur. Phys. J. A* **39**, 219 (2009); B. Gebremariam, T. Duguet, and S. K. Bogner, *Phys. Rev. C* **82**, 014305 (2010).
- [23] J. E. Drut and L. Platter (unpublished).